ISPRS Journal of Photogrammetry and Remote Sensing 64 (2009) 335–344

Contents lists available at ScienceDirect

ISPRS Journal of Photogrammetry and Remote Sensing

journal homepage: www.elsevier.com/locate/isprsjprs

Review article

Thermal infrared remote sensing for urban climate and environmental studies: Methods, applications, and trends

Qihao Weng *

Center for Urban and Environmental Change, Department of Geography, Geology, and Anthropology, Indiana State University, Terre Haute, IN 47809, USA

ARTICLE INFO

Article history:
Received 7 November 2008
Received in revised form
5 February 2009
Accepted 29 March 2009
Available online 5 May 2009

Keywords:
Thermal infrared remote sensing
Urban climate
Urban environments
Land surface temperature
Scale

ABSTRACT

Thermal infrared (TIR) remote sensing techniques have been applied in urban climate and environmental studies, mainly for analyzing land surface temperature (LST) patterns and its relationship with surface characteristics, assessing urban heat island (UHI), and relating LSTs with surface energy fluxes to characterize landscape properties, patterns, and processes. This paper examines current practices, problems, and prospects in this particular field of study. The emphasis is placed in the summarization of methods, techniques, and applications of remotely sensed TIR data used in urban studies. In addition, some future research directions are outlined. This literature review suggests that the majority of previous research have focused on LST patterns and their relationships with urban surface biophysical characteristics, especially with vegetation indices and land use/cover types. Less attention has been paid to the derivation of UHI parameters from LST data and to the use of remote sensing techniques to estimate surface energy fluxes. Major recent advances include application of sub-pixel quantitative surface descriptors in examining LST patterns and dynamics, derivation of key UHI parameters based on parametric and non-parametric models, and integration of remotely sensed variables with *in situ* meteorological data for urban surface energy modeling. More research is needed in order to define better "urban surface" from the remote sensing viewpoint, to examine measurement and modeling scales, and to differentiate modeled and measured fluxes.

1. Introduction

Remotely sensed thermal infrared (TIR) data have been widely used to retrieve land surface temperature (LST) (Quattrochi and Luvall, 1999; Weng et al., 2004). A series of satellite and airborne sensors have been developed to collect TIR data from the earth surface, such as HCMM, Landsat TM/ETM+, AVHRR, MODIS, ASTER, and TIMS. In addition to LST measurements, these TIR sensors may also be utilized to obtain emissivity data of different surfaces with varied resolutions and accuracies. LST and emissivity data are used in urban climate and environmental studies, mainly for analyzing LST patterns and its relationship with surface characteristics, for assessing urban heat island (UHI), and for relating LSTs with surface energy fluxes in order to characterize landscape properties, patterns, and processes (Quattrochi and Luvall, 1999).

LST is an important parameter in the studies of urban thermal environment and dynamics. LST modulates the air temperature of the lower layer of urban atmosphere, and is a primary factor in determining surface radiation and energy exchange, the internal climate of buildings, and human comfort in the cities (Voogt and Oke, 1998). The physical properties of various types of urban surfaces, their color, the sky view factor, street geometry, traffic loads, and anthropogenic activities are important factors that determine LSTs in the urban environments (Chudnovsky et al., 2004). The LST of urban surfaces correspond closely to the distribution of land use and land cover (LULC) characteristics (Lo et al., 1997; Weng, 2001, 2003; Weng et al., 2004). To study urban LSTs, some sophisticated numerical and physical models have been developed, including energy balance models (Oke et al., 1999; Tong et al., 2005), laboratory models (Cendese and Monti, 2003), three-dimensional simulations (Saitoh et al., 1996), Gaussian models (Streutker, 2002), and other numerical simulations. Among these models and simulations, statistical analysis plays an important role in linking LST to the surface characteristics, especially at larger geographical scales (Bottyán and Unger, 2003). Previous studies had linked LST with biophysical and meteorological factors, such as built-up area and height (Bottyán and Unger, 2003), urban and street geometry (Eliasson, 1996), LULC (Dousset and Gourmelon, 2003), vegetation (Weng et al., 2004), as well as population distribution (Fan and Sailor, 2005; Weng et al., 2006; Xiao et al., 2008) and the intensity of

* Tel.: +1 812 237 2255; fax: +1 812 237 8029.
E-mail address: qweng@indstate.edu.

0924-2716/$ – see front matter
doi:10.1016/j.isprsjprs.2009.03.007

human activities (Elvidge et al., 1997). However, the relationship between LST and various vegetation indices has been most extensively documented in the literature.

Remotely sensed TIR data are a unique source of information to define surface heat islands, which are related to canopy layer heat islands. In situ data (in particular, permanent meteorological station data) offer high temporal resolution and long-term coverage but lacks spatial details. Moving observations overcome this limitation to some extent, but do not provide a synchronized view over a city. Only can remotely sensed TIR data provide a continuous and simultaneous view of the whole city, which is of prime importance for detailed investigation of urban surface climate. Rao (1972) was the first to assess the possibility of detection of thermal footprint of urban areas. Since then, a wide range of TIR sensors have been employed to study LST and UHI by offering improvements over their ancestors. However, among many of the previous studies, there is confusion between LST patterns and UHIs. The concept of a "satellite-derived" heat island is largely an artifact of low spatial resolution imagery used, and the term "surface temperature patterns" is more meaningful than surface heat island (Nichol, 1996). It remains to be a valid scientific issue of how satellite-derived LSTs can be utilized to derive UHI parameters and to model and to simulate the UHI over the space and time.

Three items of information are needed in order to estimate land surface energy fluxes: (1) energy driving forces (i.e., incident solar energy, albedo, and resulting net radiation), (2) soil moisture availability and the vegetation–soil interaction; and (3) capacity of the atmosphere to absorb the flux, which depends on surface air temperature, vapor pressure gradients and surface winds (Schmugge et al., 1998). Previous works have focused on the methods for estimating variables related to the first two items from satellite remote sensing data, but little has been done to estimate the surface atmospheric parameters (Schmugge et al., 1998). These parameters are measured in the traditional way in the network of meteorological stations or *in situ* field measurements. Generally speaking, the application of TIR data has been limited in urban surface energy modeling (Voogt and Oke, 2003). This limitation is due primarily to the perceived difficulty in the use and availability of TIR data and the fragmentation of references on thermal remote sensing in the literature (Quattrochi and Luvall, 1999).

This paper examines methods and applications in current practices of applying TIR data to urban climate and environmental studies. The emphasis is placed in the summarization of major advances and problems in LST retrieval, the LST–vegetation relationship, and UHI studies with remotely sensed TIR data and with the energy balance modeling. In the last part of the paper, the author would share his viewpoint on research trends in thermal remote sensing of urban areas, and would provide updates on current and future TIR remote sensors.

2. LST retrieval and key parameters

2.1. LST retrieval

Satellite TIR sensors measure top of the atmosphere (TOA) radiances, from which brightness temperatures (also known as blackbody temperatures) can be derived using Plank's law (Dash et al., 2002). The TOA radiances are the mixing result of three fractions of energy: (1) emitted radiance from the Earth's surface, (2) upwelling radiance from the atmosphere, and (3) downwelling radiance from the sky. The difference between the TOA and land surface brightness temperatures ranges generally from 1 K to 5 K in the 10–12 μm spectral region, subject to the influence of the atmospheric conditions (Prata et al., 1995). Therefore, atmospheric effects, including absorption, upward emission, and downward irradiance reflected from the surface (Franca and Cracknell, 1994), must be corrected before land surface brightness temperatures are obtained. These brightness temperatures should be further corrected with spectral emissivity values prior to the computation of LST to account for the roughness properties of the land surface, the amount and nature of vegetation cover, and the thermal properties and moisture content of the soil (Friedl, 2002). Two approaches have been developed to recover LST from multispectral TIR imagery (Schmugge et al., 1998). The first approach utilizes a radiative transfer equation to correct the at-sensor radiance to surface radiance, followed by an emissivity model to separate the surface radiance into temperature and emissivity (Schmugge et al., 1998). The second approach applies the split-window technique for sea surfaces to land surfaces, assuming that the emissivity in the channels used for the split window is similar (Dash et al., 2002). Land surface brightness temperatures are then calculated as a linear combination of the two channels. A major disadvantage of this approach is that the coefficients are only valid for the datasets used to derive those (Dash et al., 2002). In other words, a set of thermal responses for a specific landscape phenomenon or process measured using a particular TIR sensor cannot be extrapolated to predict the same TIR measurements either from other sensors, or from images recorded at different times using the same sensor (Quattrochi and Goel, 1995).

Less attention has been paid to develop methods of LST retrieval from a single-channel TIR data, such as Landsat TM/ETM+ TIR band. Sobrino et al. (2004) examined three different single-channel methods, including: the radiative transfer equation using *in situ* radiosounding data; the mono-window algorithm (Qin et al., 2001); and the single-channel algorithm (Jiménez-Muñoz and Sobrino, 2003). The error sources that impact the accuracy of LST estimation with the radiative transfer equation may come from atmospheric correction, noise of the sensor, land surface emissivity, aerosols and other gaseous absorbers, angular effects, wavelength uncertainty, full-width at half-maximum of the sensor, and band-pass effects (Jiménez-Muñoz and Sobrino, 2006). The most significant sources of error, however, are associated with atmospheric effects, which may introduce an error on the estimation ranging from 0.2 K to 0.7 K, and with land surface emissivity, which can produce an error up to 0.2 K to 0.4 K (Jiménez-Muñoz and Sobrino, 2006). The above algorithms have not been frequently referenced and applied in urban climate and environmental studies as they are deserved. The majority of urban studies are interested in relative LST measurements, i.e., in mapping the spatial variations of LST and/or environmental modeling with relative LSTs. A widely used method results from the *Landsat-7 Science Data User's Handbook*, developed by the Landsat Project Science Office at NASA's Goddard Space Flight Center (Landsat Project Science Office, 2002). After converting the digital numbers (DN) of the Landsat ETM+ Band 6 into absolute radiance values, at-satellite brightness temperatures (i.e., blackbody temperature) are computed under the assumption of unity emissivity and using pre-launch calibration constants, which is followed by a correction for spectral emissivity according to the nature of land cover/use (Weng et al., 2004). Most urban studies found this straightforward approximation sufficient, which replaced the sensor response function with a delta function at the sensor's central wavelength to invert LSTs with the assumption of uniform emissivity (Weng et al., 2006; Lu and Weng, 2006).

2.2. Emissivity

The effect of land surface emissivity on satellite measurements can be generalized into three categories: (1) emissivity causes a reduction of surface-emitted radiance; (2) non-black surfaces reflect radiance; and (3) the anisotropy of reflectivity and

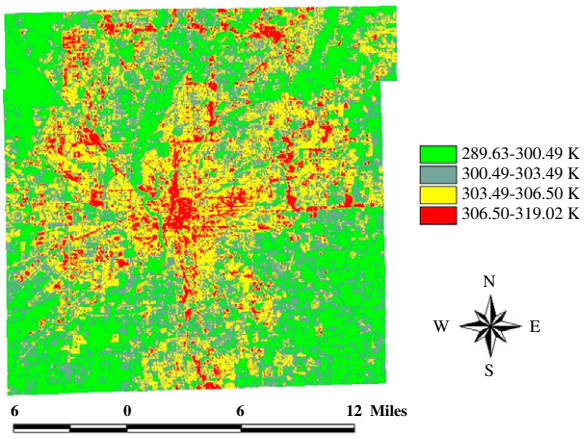

Fig. 1. Emissivity-corrected LST map of Indianapolis, United States. LSTs were derived from a Landsat ETM+ thermal infrared image of June 22, 2000. (Source: Weng et al., 2004).

emissivity may reduce or increase the total radiance from the surface (Prata, 1993). Therefore, retrieval of LST from multispectral TIR data requires an accurate measurement of emissivity values of the surface (Caselles et al., 1995). The emissivity of a surface is controlled by such factors as water content, chemical composition, structure, and roughness (Snyder et al., 1998). For vegetated surfaces, emissivity can vary significantly with plant species, areal density, and growth stage (Snyder et al., 1998). In the mean time, emissivity is a function of wavelength, commonly referred to as spectral emissivity (Dash et al., 2002). Emissivity for ground objects from passive sensor data has been estimated using different techniques. Among those techniques are the normalized emissivity method (Gillespie, 1985), thermal spectral indices (Becker and Li, 1990), spectral ratio method (Watson, 1992), Alpha residual method (Kealy and Gabell, 1990), NDVI method (Valor and Cassells, 1996), classification-based estimation (Snyder et al., 1998), and the temperature-emissivity separation method (Gillespie et al., 1998; Liang, 2001). The above techniques are applicable to separate temperature from emissivity, so that the effect of emissivity on estimated LST can be determined. Lack of knowledge of emissivity can introduce an error ranging from 0.2 K to 1.2 K for mid-latitude summers and from 0.8 K to 1.4 K for the winter conditions for an emissivity of 0.98 and at the ground height of 0 km, when a single-channel method of LST estimation is used (Dash et al., 2002). Moreover, it may not be practical to measure emissivity values pixel-by-pixel, since numerous factors are involved. Snyder et al. (1998) proposed to use kernel methods applied to three bidirectional reflectance distribution function (BRDF) models (a geometric model for sparse vegetation, a volumetric model for dense vegetation, and a specular model for water and ice), so that each pixel can be categorized into one of the fourteen emissivity classes based on conventional land cover classification and seasonal factors. Fig. 1 shows emissivity-corrected LST map of Indianapolis, United States. LSTs were derived from a Landsat ETM+ thermal infrared image of June 22, 2000, by employing the emissivity correction scheme of Snyder et al. (1998).

2.3. Vegetation abundance and soil properties

Fractional vegetation cover depicts the amount and nature of vegetation cover, and modulates the proportions of vegetation and non-vegetated ground (e.g., bare soil) visible to a sensor. The differences in radiative temperature between the vegetation canopy and the ground affect the measurement of LST (Sandholt et al., 2002). For non-vegetated areas, LST measurements typically represent the radiometric temperatures of sunlit non-vegetated surfaces, such as bare soil. As the amount of vegetation cover increases, the radiative temperature recorded by a sensor approximates more closely the temperatures of green leaves, and the canopy temperature at spectral vegetation maximum or complete canopy cover (Goward et al., 2002). It is of significance to scrutinize the temperatures of each part of the vegetation–ground system (such as shaded ground, sunny ground, shade vegetation, and sunny vegetation) and to examine the effects of different canopy structures (Kimes, 1983; Cassells et al., 1992a,b). In general, for image pixels that are not completely occupied by a single homogeneous vegetation or bare soil, LST measurements reflect a mixture of ground and vegetation canopy temperatures, resulting from a composite signature. The observed portion of ground and vegetation can vary with the viewing angle, thus the amount of vegetation (ground) alters as the observation angle increases (Cassells et al., 1992a). In addition, LST measurement will also be subject to the influences of the lower atmosphere and the temperature difference between the vegetation canopy and the soil background (Friedl, 2002). Thermal responses for vegetation can be highly varied as a function of the biophysical properties of the vegetation itself as well (Quattrochi and Ridd, 1998).

For any surface material, certain internal properties, such as heat capacity, thermal conductivity and inertia, play important roles in governing the temperature of a body at equilibrium with its surroundings (Campbell, 2002). These thermal properties vary with soil type and its moisture content (Sandholt et al., 2002). Dry, bare, and low-density soils, for example, have been linked to high LST as a result of relatively low thermal inertia (Carnahan and Larson, 1990). The emissivity of soils is a function of soil moisture conditions and soil density (Larson and Carnahan, 1997). Therefore, for the areas characterized by partial vegetation cover, surface thermal properties can largely influence the measurement of LST through the thermal processes of conduction, convection, and radiation.

3. Relationship between LST and vegetation abundance

The relationship between LST and vegetation indices, such as NDVI, has been extensively documented in the literature. For example, the LST–vegetation index relationship has been used by Carlson et al. (1994) to retrieve surface biophysical parameters, by Kustas et al. (2003) to extract sub-pixel thermal variations, and by Lambin and Ehrlich (1996) and Sobrino and Raissouni (2000) to analyze land cover dynamics. Many studies observed a negative relationship between LST and vegetation indices. This finding had stimulated research into two major directions, i.e., statistical analysis of the LST–vegetation abundance relationship and the TVX (thermal-vegetation index) approach. TVX is a multispectral method of combining LST and a vegetation index in a scatter plot to observe their associations (Quattrochi and Ridd, 1994).

3.1. Statistical analysis of the LST–vegetation abundance relationship

To understand the statistical relationship between LST and vegetation cover, different vegetation indices have been employed in search of a representative index. Goward et al. (2002) showed different spectral vegetation indices such as NDVI and simple ratio were related to LAI (leaf area index) and green biomass. For a long time, NDVI were used to quantify vegetation patterns and dynamics within the cities, and has been incorporated with LST to measure the impacts of urbanization (Weng and Lu, 2008). The relationship between NDVI and fractional vegetation cover is not singular, however. Small (2001) suggested that NDVI did not provide the areal estimates of the amount of vegetation. NDVI measurements are a function of the visible and near-infrared reflectance from plant canopy, the reflectance of the same spectra

from the soil, and the atmospheric reflectance, and are subject to the influence of an error related to observational and other errors (Yang et al., 1997). Plant species, leaf area, soil background, and shadow can all contribute to the NDVI variability (Jasinski, 1990). The relationship between NDVI and other measures of vegetation abundance (e.g., LAI values of greater than 3) is well known to be nonlinear (Asrar et al., 1984). This nonlinearity and the platform dependency suggest that NDVI may not be a good indicator for quantitative analyses of vegetation (Small, 2001), and the relationship between NDVI and LST needs further calibration. More quantitative, physically-based measures of vegetation abundance are called for, especially for applications that require biophysical measures (Small, 2001). The importance of spatial resolution for detecting landscape patterns and changes should also be emphasized (Frohn, 1998), and the relationship between NDVI variability and pixel size should be further investigated (Jasinski, 1990).

More recent investigations have been directed to find a surrogate to NDVI. Weng et al. (2004) derived vegetation fraction at different scales (pixel aggregation levels), made a comparison between NDVI and vegetation fraction in terms of their effectiveness as an indicator of urban thermal patterns, and found a stronger negative correlation between vegetation fraction and LST than that between NDVI and LST. Yuan and Bauer (2007) made a similar correlation analysis between impervious surface area (ISA) and NDVI, and suggested that ISA showed higher stability and lower seasonal variability and thus recommended it as a complementary measure to NDVI. Xian and Crane (2006) supported the above observations by suggesting that the combined use of ISA, NDVI and LST can explain temporal thermal dynamics across the cities.

3.2. The TVX approach to the LST–vegetation relationship

The combination of LST and NDVI by a scatter plot results in a triangular shape (Carlson et al., 1994; Gillies and Carlson, 1995; Gillies et al., 1997). Several methods have been developed to interpret the LST-NDVI space, including: (1) the "triangle" method using soil–vegetation–atmosphere transfer (SWAT) model (Carlson et al., 1994; Gillies and Carlson, 1995; Gillies et al., 1997); (2) *in situ* measurement method (Friedl and Davis, 1994); and (3) remote-sensing-based method (Betts et al., 1996). However, difficulties still exist in interpretation of LST for sparse canopies because the measurements have combined the temperature of the soil and that of the vegetation, and the combinations are often nonlinear (Sandholt et al., 2002). Different versions of the TVX approach had been developed during the past decades. Price (1990) found that radiant surface temperature showed more variations in sparse vegetated areas than in densely vegetated areas. This behavior results in the atypical triangular shape or as observed by Moran et al. (1994) in a trapezoid shape for large heterogeneous regions under strongly sunlit conditions (Gillies et al., 1997).

Carlson (2007) recently provided a comprehensive review of the "Triangle Method" for estimating surface evapotranspiration and soil moisture. Fig. 2 shows an example of Fr/T* scatter plot with sample LULC classes from a Landsat TM image of the city of Tabriz (38°05′, 46°17′) in the northwestern Iran, which was acquired on August 2, 2001. To create the plot, cloud contaminated pixels were first excluded. NDVI values were re-scaled between bare soil ($NDVI_0$) and dense vegetation ($NDVI_S$) followed a method by Owen et al. (1998). Fractional vegetation cover (Fr) was then calculated as the square of the re-scaled value N*. Areas with high and low temperatures (T_{max} and T_0) were selected from the bare and wet soils respectively, and their data were used to calculate the normalized temperature values of T* (Gillies et al., 1997). The resulted Fr/T* scatter plot showed a typical triangular pattern, with a clear "warm edge" defined by the right side of the pixel envelope.

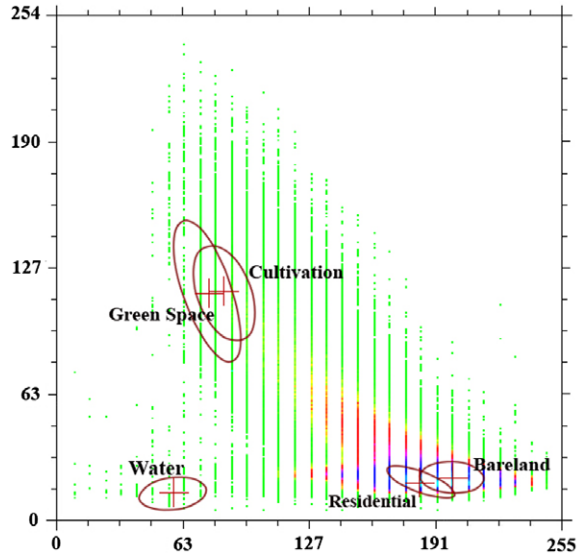

Fig. 2. Fr/T* scatter plot with sample LULC classes from a Landsat TM image of the city of Tabriz (38°05′, 46°17′) in the northwestern Iran, which was acquired on August 2, 2001. To create the plot, cloud contaminated pixels were first excluded. NDVI values were re-scaled between bare soil ($NDVI_0$) and dense vegetation ($NDVI_S$) followed a method by Owen et al. (1998). Fractional vegetation cover (Fr) was then calculated as the square of the rescaled value N*. Areas with high and low temperatures (T_{max} and T_0) were selected from the bare and wet soils respectively, and their data were used to calculate the normalized temperature values of T* (Gillies et al., 1997). The resulted Fr/T* scatter plot showed a typical triangular pattern, with a clear "warm edge" defined by the right side of the pixel envelope. (Source: Amiri et al., 2008).

The slope of the LST-NDVI curve has been related to soil moisture conditions (Carlson et al., 1994; Gillies and Carlson, 1995; Gillies et al., 1997; Goetz, 1997; Goward et al., 2002), the evapotranspiration of the surface (Boegh et al., 1998), and other applications in shaping the TVX concept. Ridd (1995) and Carlson et al. (1994) interpreted different sections of the triangle and related them to different LULC types. Lambin and Ehrlich (1996) presented a comprehensive interpretation of the TVX space, while Carlson and Arthur (2000) gave a physical meaning to the space. Furthermore, Goward et al. (2002) provided a detailed analysis of the underlying biophysics of the observed TVX relationship, and suggested that the relationship was the result of modulation of radiant surface temperature by vegetation cover.

The TVX approach was the subject of the studies focusing on the development of new applications, and the patterns and dynamics of different vegetation types at the scales from local to global. Researchers used the TVX concept to develop new indices and estimated parameters. Moran et al. (1994) used the TVX trapezoid to develop a new index called water deficit index (WDI) to estimate evapotranspiration in the lack of meteorological data using the surface minus air temperature. Lambin and Ehrlich (1996) proposed radiant surface temperature - NDVI ratios in the TVX space, and showed its usefulness in land cover mapping. Owen et al. (1998) used the same space and suggested a land cover index (LCI) for assessing UHI. Carlson and Arthur (2000) extended the TVX approach to calculate impervious surface area and surface runoff. Jiang and Islam (2001), by using linear decomposition of TVX scatter plot, estimated the "α" parameter of the Priestly–Taylor equation in the absence of ground meteorological data. Sandholt et al. (2002) proposed a temperature–vegetation dryness index (TVDI) based on the relationship between surface temperature and NDVI, and showed the effectiveness of TVDI by explaining

larger spatial variations than hydrological models. Nishida et al. (2003) estimated evapotranspiration fraction (EF) using a new TVX algorithm to provide global time-series coverage of EF from MODIS data. Chen et al. (2006) investigated the relationship between temperature and various newly developed indices, and found that NDVI presented a limited range.

Apart from the introduction of new indices, much research has been carried out in the extraction of new TVX metrics. Several studies have focused on the slope of the LST – NDVI fit line (Nemani and Running, 1989; Smith and Choudhury, 1991). Variations in the slope and intercept of the TVX space have been interpreted in relation to surface parameters. Nemani and Running (1989) related the slope of the TVX correlation to the stomatal resistance and the evapotranspiration in a deciduous forest. Sandholt et al. (2002) linked TVX correlation slope to the evapotranspiration rate and used the relationship to estimate air temperature.

The TVX concept has further been used to perform pixel trajectories. The idea has been emerging over the past decade that land surface parameters associated with individual pixels can be visualized as vectors tracing out paths in multi-parameter space (Lambin and Ehrlich, 1996). Several studies identified urbanization as the major cause of the observed migration within the TVX space (Owen et al., 1998); (Carlson and Sanchez-Azofeifa, 1999). Owen et al. (1998) found that the initial location of the migrating pixels in the TVX triangle determined the magnitude and direction of the path. Carlson and Sanchez-Azofeifa (1999) used the TVX method to assess how surface climate was affected by rapid urbanization and deforestation in San Jose, Costa Rica. They found that urbanization was more effective than the latter, and that different development styles followed different paths in the space. Carlson and Arthur (2000) compared average trajectories of different development styles, and showed that in advanced stages of development, the paths became closer and indistinguishable.

Finally, the TVX approach has been used in the so-called Triangle Inversion Method to derive surface parameters. Carlson et al. (1994) used a Soil–Vegetation–Atmosphere Transfer (SVAT) model to show feasibility of the extraction of surface parameters such as soil moisture content and fractional vegetation cover (Fr) from the analysis of the TVX space without ground data. This inversion method was used to impose physical limits on a solution of SVAT model parameterized for a test site to remote variables used in the model to derive surface biophysical variables. Gillies et al. (1997) verified that the borders of the triangle constrained the solutions for determining the surface energy fluxes. Goward et al. (2002) used the TVX approach as a mean for the assessment of soil moisture conditions from satellite data. Owen et al. (1998) used this method to assess the impacts of urbanization on the surface parameters.

Some authors, however, have drawn attention to the problems of the TVX space. Goward et al. (2002) showed that the impact of plant stomatal function confused the interpretation of the TVX space given by experimental studies to use TVX slope to assess soil moisture conditions. Nishida et al. (2003) discussed four main difficulties with the TVX method for ET estimation. The problems included: (1) its dependency on meteorological data, (2) computational difficulties of inversion of numerical models in global scale, (3) problem of accurate estimation in dense vegetation, and (4) difficulties of estimation in complex landscapes. While trying to establish guidelines to overcome the above problems by a new model, they suggested that their model was effective for urbanization monitoring since EF was able to capture variations in surface energy partitioning (Nishida et al., 2003).

4. Remote sensing of urban heat islands

4.1. The energy balance approach

Knowledge of urban surface energy balance is fundamental to understanding of UHIs and urban thermal behavior (Oke, 1982, 1988). If the net horizontal heat advection is not considered, the surface energy balance of a city can be expressed as:

$$R_n + A = H + LE + G \ (\mathrm{W\ m^{-2}}) \quad (1)$$

where R_n is the net all-wave radiation, A the anthropogenic heat flux, H the sensible heat flux, LE the latent heat flux, and G the net storage heat flux. Oke (1988) gave a comprehensive review of the energy balance approach and its development as applied to urban areas. The most recent developments were reviewed by Piringer et al. (2002) and Grimmond (2006). To quantify the urban surface energy balance, *in situ* measurements (largely tower-based) can be obtained to estimate accurate heat fluxes at the roof level. However, because the diversity of size, shape, height, composition, and the spatial arrangement of urban 'canopy' components, it is difficult to define a surface datum for such measurements, especially for an entire city (Oke, 1988). Moreover, the sites of the measurements are frequently not associated with meteorological stations (Piringer et al., 2002). To date, most of the urban heat flux observations have been conducted in a limited number of residential areas (Grimmond and Oke, 1995). Several experimental studies were conducted in European cities, but did not analyze specifically the different components of surface energy balance (Piringer et al., 2002). Because direct observation of heat fluxes is rare, many efforts have been made to parameterize the terms by using more routinely measured data (e.g., (Grimmond and Oke, 2002; Offerle et al., 2005; Holt and Pullen, 2007). Grimmond et al. (2008) conducted a comprehensive comparison among thirty-five models of urban surface energy balance in terms of model characteristics and methodology. Furthermore, because much of the work conducted in the past were by individuals or small groups for their own cities, there is a need to develop inventories of the projects and metadata about study sites, instrumentation, and data processes (Grimmond, 2006).

A fundamental problem with the *in situ* measurements of energy fluxes lies in the great difficulty of selecting a representative site for a larger adjacent region, due to the complexity of urban material composition. Grimmond and Souch (1994) outlined the method to extract surface cover information for the Multi-city Urban Hydrometeorological Database (MUHD). The most noticeable recent advance in terms of instrumentation relates to the use of stand-alone sensors, with which observational data can be recorded for a network in a city (Grimmond, 2006). Even with the MUHD and the new sensor technology, siting criteria for urban locations are still hard to define for documenting local-scale heat flux variability. It is extremely difficult and expensive to investigate the detailed spatial pattern of energy fluxes in a city, if cost, time, instrument and data calibrations are considered all together. Furthermore, the surface energy balance approach has met with mixed success in documenting the temporal variability of energy fluxes in urban areas. Most of the *in situ* measurements are used to determine the diurnal variability, but less used for evaluating the seasonal and the inter-year variability.

4.2. The remote sensing approach

Previous studies of urban thermal landscapes and UHIs have been conducted by using NOAA AVHRR data (Kidder and Wu, 1987; Balling and Brazell, 1988; Roth et al., 1989; Gallo et al., 1993; Gallo and Owen, 1998; Streutker, 2002)). However, for all

of these studies, the 1.1 km spatial resolution AVHRR data were found suitable only for large-area urban temperature mapping, not for establishing accurate and meaningful relationships between image-derived values and those measured on the ground. The 120 m resolution Landsat TM (and later ETM+ data of 60 m) TIR data have also been extensively utilized to derive LSTs and to study UHIs. Carnahan and Larson (1990) used the TM TIR data to observe meso-scale temperature differences between the urban and rural areas in Indianapolis, while Kim (1992) studied similar phenomena in Washington, DC. Nichol (1994) utilized TM TIR data to monitor microclimate for housing estates in Singapore, and further calculated LSTs of building walls based on a 3-D GIS model (Nichol, 1998). Weng (2001, 2003) examined LST pattern and its relationship with land cover in Guangzhou and in the urban clusters in the Pearl River Delta of China. Weng et al. (2004) utilized a Landsat ETM+ image to examine the LST–vegetation abundance relationship in Indianapolis. More recently, Lu and Weng (2006) applied spectral mixture analysis (SMA) to ASTER images to derive hot-object and cold-object fractions from the TIR bands of the sensor and biophysical variables from non-thermal bands. Statistical analyses were then conducted to examine the relationship between LST and the derived fraction variables across the resolution from 15 m to 90 m.

Studies using satellite-derived LSTs have been termed as the surface temperature UHI (Streutker, 2002). Moreover, satellite-derived LSTs are believed to correspond more closely with the canopy layer heat islands, although a precise transfer function between LST and the near ground air temperature is not yet available (Nichol, 1994). Voogt and Oke (2003) criticized that thermal remote sensing of urban areas had been slowly progressed due largely to qualitative description of thermal patterns and simple correlations between LST and LULC types since 1989, when Roth et al. (1989) was published in *International Journal of Remote Sensing*. Xiao et al. (2008) further noticed that little research has been done on the statistical relationship between LST and non-biophysical factors.

Most recent advances include development and utilization of quantitative surface descriptors for assessing the interplay between urban material fabric and urban thermal behavior (Weng et al., 2004, 2006; Lu and Weng, 2006; Weng and Lu, 2008). Moreover, the landscape ecology approach had been employed to assess this interplay across various spatial resolutions and to identify the operational scale where both LST and LULC processes interacted to generate the urban thermal landscape patterns (Weng et al., 2007; Liu and Weng, 2008). Because ASTER sensor collects both daytime and nighttime TIR images, analysis of LST spatial patterns has also been conducted for a diurnal contrast (Nichol, 2005).

A key issue in the application of TIR remote sensing data in urban climate studies is how to use LST measurements at the micro-scale to characterize and quantify UHIs observed at the meso-scale. Streutker (2002, 2003) used AVHRR data to quantify the UHI of Houston, Texas, as a continuously varying two-dimensional Gaussian surface superimposed on a planer rural background, and derive the UHI parameters of magnitude (i.e., intensity), spatial extent, orientation, and central location. Rajasekar and Weng (2009) applied a non-parametric model by using fast Fourier transformation (FFT) to MODIS imagery for characterization of the UHI over space, so as to derive UHI magnitude and other parameters. Fig. 3 shows selected models of the daytime UHIs characterized from the MODIS LST images of 2006 in Indianapolis, Indiana, United States. In spite of these advances, new methods for estimation of UHI parameters from multi-temporal and multi-location TIR imagery are still needed given the increased interest in urban climate community to use remote sensing data.

Another fundamental way that TIR data can be applied is to relate LSTs with surface energy fluxes for characterizing landscape properties, patterns, and processes (Quattrochi and Luvall, 1999). Remotely sensed TIR imagery has the advantage of providing a time-synchronized dense grid of temperature data over a whole city, while optical sensing data have been used to monitor discrete land cover types and to estimate biophysical variables (Steininger, 1996). Together, remote sensing data can be used to estimate surface parameters related to the soil–vegetation system and surface soil moisture, radiation forcing components and indicators of the surface response to them (i.e., LST) (Schmugge et al., 1998). If the advantage of time-sequential observations of satellite sensors (some sensors can even scan a specific geographic location twice a day, at day and night) is considered, remote sensing data have great potentials for studying the urban surface energy budget, as well as the spatial pattern and temporal dynamics of urban thermal landscapes.

The needs are obvious in urban climate studies for the combination of the energy balance and remote sensing approaches. One of the earliest studies, which combined the surface energy modeling and remote sensing approaches, was conducted by Carlson et al. (1981). They used satellite temperature measurements in conjunction with a one-dimensional boundary layer model to analyze the spatial patterns of turbulent heat fluxes, thermal inertia, and ground moisture availability in Los Angeles and St. Louis. This method was later applied to Atlanta by using AVHRR data, in which the net urban effect was determined as the difference between the urban and rural simulations (Hafner and Kidder, 1999). Because analyses of surface energy flux are extensively conducted over vegetated and agricultural areas, successful methods have been applied to urban areas (Zhang et al., 1998; Chrysoulakis, 2003). Zhang et al. (1998) used Landsat TM data, in conjunction with routine meteorological data and field measurements, to estimate the urban surface energy fluxes in Osaka, Japan, and to analyze their spatial variability in both summer and winter. Chrysoulakis (2003) used ASTER imagery, together with *in situ* spatial data, to determine the spatial distribution of all-wave surface net radiation balance in Athens, Greece. Kato and Yamaguchi (2005) combined ASTER and Lansat ETM+ data with ground meteorological data to investigate the spatial patterns of surface energy fluxes in Nagoya, Japan, in four distinct seasons by separating anthropogenic heat discharge and natural heat radiation from sensible heat flux.

5. Prospects

To understand better urban thermal landscapes and UHIs, and to promote related urban environmental research, some key issues need to be addressed. The most fundamental issue is the definition of "urban surface", since remote sensors see the Earth's surface in plan-view (Roth et al., 1989). The effective radiometric source area of a remote sensing measurement is the instantaneous field of view of the sensor projected onto the earth's surface, and is subject to the effect of sensor viewing geometry and surface structure (Voogt and Oke, 2003). The energy balance and thus LST are controlled by such surface characteristics as albedo, surface roughness, soil thermal inertia, and soil moisture (Hafner and Kidder, 1999). The remote sensing approach should continue to define and estimate appropriate parameters from remote sensors to describe better the urban surface and to apply to urban atmospheric models (Voogt and Oke, 2003). Soil thermal inertia and moisture are two significant parameters in determining the surface energy balance in urban areas (Piringer et al., 2002).

Equally important is the issue of measurement and modeling scale. It should not be assumed that a set of thermal responses for a specific landscape or process using a specific TIR sensor can be used to predict the same TIR measurements either from

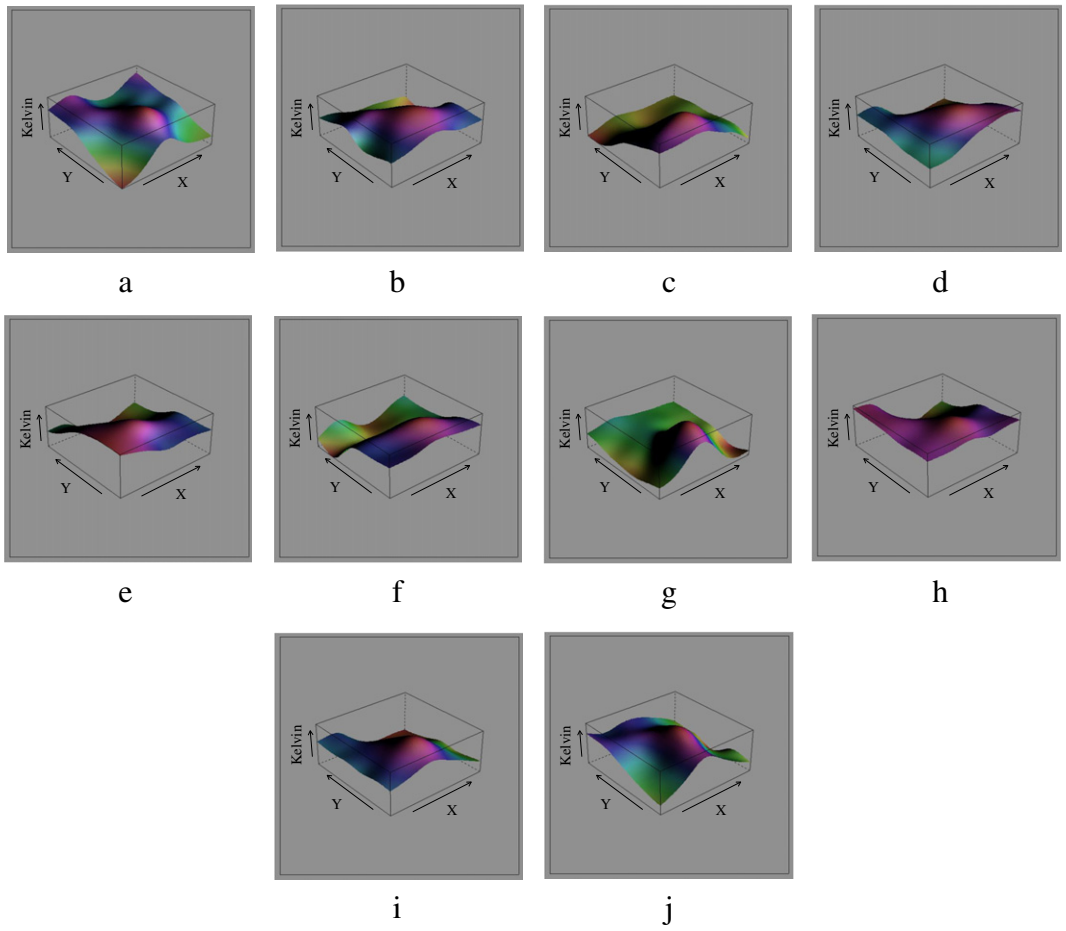

Fig. 3. Selected models of the daytime UHIs characterized from the MODIS LST images of 2006 in Indianapolis, United States. The modeled UHIs were constructed with a non-parametric modeling technique by using fast Fourier transformation. The models from (a) to (j) are derived from the following dates of images: February 18, March 15, April 14, May 24, June 24, July 9, August 21, September 30, October 4, and November 11. (Source: Rajasekar and Weng, 2009).

other sensors or from images recorded at different times using the same sensor (Quattrochi and Goel, 1995). The complex relationship requires detailed research between the observational scale of a remote sensor (pixel resolution) and the operational scale, where operational processes as reflected in the remote sensing imagery interact to govern the landscape patterns and environmental processes (Weng et al., 2007; Liu and Weng, 2008). This relationship is especially important for complex, heterogeneous landscapes such as urban thermal landscapes. Schmid (1988) found that the directional variations of thermal radiance (i.e., effective anisotropy) could remain constant over a range of scales, which correspond to areas of similar urban structures that generate the regional homogeneity of LST, but the lower bound of the range may be 25 m (street/alley to house row spacing), 50 m (street to alley spacing), and up to 200 m in diameter. Urban surface anisotropy is expected to stay relatively constant as the scale increases up to the limit where ground resolution begins to cover different land uses or surface structures, and the scale ranges from approximately 12 m to 1000 m (Voogt and Oke, 1998). Weng et al. (2004) found the operational scale to be 120 m in assessing the LST–vegetation abundance relationship of the City of Indianapolis, U.S.A. It is expected the operational scale would vary from city to city depending upon the biophysical and anthropogenic settings of a city.

Finally, a better understanding of the differences between modeled and measured fluxes is essential. The IFOVs of remote sensors generally do not match with the source area associated with surface flux measurements, which are typically collected using eddy correlation or Bowen-ratio energy balance instruments, and measured flux quantities reflect processes that have been partially integrated with the near-surface atmosphere over the upwind fetch typical of hundreds of meters (Friedl, 2002). Close cooperation between energy balance modelers, field workers, and remote sensing scientists would facilitate the research on the linkage among LST, the surface energy balance, and air temperature in the above the urban canopy layer.

Urban climate and environmental studies will be difficult, if not impossible, without TIR sensors of global imaging capacity. At the present, there are few sensors that have such thermal IR capabilities. The TM sensor onboard Landsat 5 has been acquiring images of the Earth nearly continuously from March 1984 to the present, with a TIR band of 120 m resolution, and is well-past the mission's life expectancy. On April 2, 2007, updates to the radiometric calibration of Landsat 5 TM data processed and distributed by the USGS EROS created an improved Landsat 5 TM data product that is now more comparable to Landsat 7 ETM+ radiometrically, and provides the basis for continued long-term studies of the Earth's land surfaces. Another TIR sensor that has global imaging capacity is with Landsat 7 ETM+. On May 31, 2003, the ETM+ Scan Line Corrector (SLC) failed permanently. Although it is still capable of acquiring useful image data with the SLC turned off, particularly within the central part of any given scene, NASA has teamed up with USGS to focus on the LDCM (Landsat Data Continuity Mission), which is most likely not to have a thermal IR imager. In addition, Terra's ASTER TIR bands of 90 m resolution have been increasingly used in urban climate and environmental studies in recent years. ASTER is an on-demand instrument, which means that data are only acquired over the requested locations.

Terra satellite launched in December 1999 as part of NASA's Earth Observing System has the life expectancy of six years, and is now also over-due.

The scientific and user community is looking forward to a Landsat ETM-like TIR sensor. The draft requirements for the LDCM thermal imager indicate that two thermal bands (10.3–11.3 μm and 11.5–12.5 μm) of 90 m or better spatial resolution are preferred (for details please refer to the LDCM web site at http://ldcm.nasa.gov/procurement/TIRimagereqs051006.pdf). The National Research Council Decadal Survey indicates the need for a similar TIR sensor. The Hyperspectral Infrared Imager (HyspIRI) is defined as a mission with Tier-2 priority, which is expected to be launched in the next 8 to10 years. Because of its hyperspectral visible and shortwave infrared bandwidths and its multispectral thermal infrared capabilities, HyspIRI will be well-suited for deriving land cover and other biophysical attributes for urban climate and environmental studies (refer to the HyspIRI web site at http://hyspiri.jpl.nasa.gov/for more information). Its TIR imager is expected to provide 7 bands between 7.5–12 μm and 1 band at 4 μm, all with 60 m spatial resolution. This TIR sensor is intended for imaging of global land and shallow water (less than 50 m in depth) with 5-day revisit at the equator (1 day and 1 night imaging). These improved capabilities would allow for a more accurate estimation of LST and emissivity, and for deriving unprecedented information on biophysical characteristics, and even socioeconomic information such as population, quality of life indicators, and human settlements. Such information cannot be obtained from current generation of satellites in orbit, such as MODIS, Landsat, or ASTER. Two major areas of application identified by the HyspIRI science team are urbanization and human health through the combined use of VSWIR and TIR data. Until then, we may have to be content with Landsat and ASTER for medium resolution TIR data and MODIS and AVHRR for coarse resolution data. It is from this perspective that international collaborations on Earth resources satellites become very important.

Acknowledgments

This research is supported by National Science Foundation (BCS-0521734) for a project entitled "Role of Urban Canopy Composition and Structure in Determining Heat Islands: A Synthesis of Remote Sensing and Landscape Ecology Approach". The author would also like to acknowledge the following individuals for their contributions to this review in various capacities: Drs. Dale Quattrochi, Rongbo Xiao, Mr. Reza Amiri, and Mr. Umamaheshwaren Rajasekar. Constructive comments and suggestions made by the anonymous reviewers helped to improve this article.

References

Amiri, R., Weng, Q., Alimohammadi, A., Alavipanah, S.K., 2008. The spatial-temporal dynamics of land surface temperatures in relation to fractional vegetation cover and land use/cover in the Tabriz urban area, Iran. Remote Sensing of Environment (under review).

Asrar, G., Fuchs, M., Kanemasu, E.T., Hatfield, J.L., 1984. Estimating absorbed photosynthetic radiation and leaf area index from spectral reflectance in wheat. Agronomy Journal 76 (22), 300–306.

Balling, R.C., Brazell, S.W., 1988. High resolution surface temperature patterns in a complex urban terrain. Photogrammetric Engineering and Remote Sensing 54 (9), 1289–1293.

Becker, F., Li, Z.-L., 1990. Temperature-independent spectral indices in TIR bands. Remote Sensing of Environment 32 (1), 17–33.

Betts, A., Ball, J., Beljaars, A., Miller, M., Viterbo, P., 1996. The land surface-atmosphere interaction: A review based on observational and global modeling perspectives. Journal of Geophysical Research 101 (D3), 7209–7225.

Boegh, E., Soegaard, H., Hanan, N., Kabat, P., Lesch, L., 1998. A remote sensing study of the NDVI-T_s relationship and the transpiration from sparse vegetation in the Sahel based on high resolution satellite data. Remote Sensing of Environment 69 (3), 224–240.

Bottyán, Z., Unger, J., 2003. A multiple linear statistical model for estimating the mean maximum urban heat island. Theoretical and Applied Climatology 75 (3-4), 233–243.

Campbell, J.B., 2002. Introduction to Remote Sensing, 3rd edition. The Guilford Press, New York.

Carlson, T.N., 2007. An overview of the so-called Triangle method for estimating surface evapotranspiration and soil moisture from satellite imagery. Sensors 7, 1612–1629.

Carlson, T.N., Arthur, S.T., 2000. The impact of land use - land cover changes due to urbanization on surface microclimate and hydrology: A satellite perspective. Global and Planetary Change 25 (1–2), 49–65.

Carlson, T.N., Dodd, J.K., Benjamin, S.G., Cooper, J.N., 1981. Satellite estimation of the surface energy balance, moisture availability and thermal inertia. Journal of Applied Meteorology 20 (1), 67–87.

Carlson, T.N., Gillies, R.R., Perry, E.M., 1994. A method to make use of thermal infrared temperature and NDVI measurements to infer surface water content and fractional vegetation cover. Remote Sensing Reviews 9 (1–2), 161–173.

Carlson, T.N., Sanchez-Azofeifa, G.A., 1999. Satellite remote sensing of land use changes in and around San José, Costa Rica. Remote Sensing of Environment 70 (3), 247–256.

Carnahan, W.H., Larson, R.C., 1990. An analysis of an urban heat sink. Remote Sensing of Environment 33 (1), 65–71.

Caselles, V., Coll, C., Valor, E., Rubio, E., 1995. Mapping land surface emissivity using AVHRR data: Application to La Mancha, Spain. Remote Sensing Review 12 (3–4), 311–333.

Cassells, V., Sobrino, J.A., Coll, C., 1992a. On the use of satellite thermal data for determining evapotranspiration in partially vegetated areas. International Journal of Remote Sensing 13 (14), 2669–2682.

Cassells, V., Sobrino, J.A., Coll, C., 1992b. A physical model for interpreting the land surface temperature obtained by remote sensors over incomplete canopies. Remote Sensing of Environment 39 (3), 203–211.

Cendese, A., Monti, P., 2003. Interaction between an inland urban heat island and a sea-Breeze flow: A laboratory study. Journal of Applied Meteorology 42 (11), 1569–1583.

Chen, X.-L., Zhao, H.-M., Li, P.-X., Yin, Z.-Y., 2006. Remote sensing image-based analysis of the relationship between urban heat island and land use/cover changes. Remote Sensing of Environment 104 (2), 133–146.

Chrysoulakis, N., 2003. Estimation of the all-wave urban surface radiation balance by use of ASTER multispectral imagery and in situ spatial data. Journal of Geophysical Research D: Atmospheres 108 (18), ACL 8-1 - ACL 8-10.

Chudnovsky, A., Ben-Dor, E., Saaroni, H., 2004. Diurnal thermal behavior of selected urban objects using remote sensing measurements. Energy and Buildings 36 (11), 1063–1074.

Dash, P., Gottsche, F.-M., Olesen, F.-S., Fischer, H., 2002. Land surface temperature and emissivity estimation from passive sensor data: Theory and practice-current trends. International Journal of Remote Sensing 23 (13), 2563–2594.

Dousset, B., Gourmelon, F., 2003. Satellite multi-sensor data analysis of urban surface temperature and land cover. ISPRS Journal of Photogrammetry and Remote Sensing 58 (1–2), 43–54.

Eliasson, I., 1996. Urban nocturnal temperatures, street geometry and land use. Atmospheric Environment 30 (3), 379–392.

Elvidge, C.D., Baugh, K.E., Kihn, E.A., Kroehl, H.W., Davis, E.R., Davis, C.W., 1997. Relation between satellite observed visible-near infrared emissions, population, economic activity and electric power consumption. International Journal of Remote Sensing 18 (6), 1373–1379.

Fan, H., Sailor, D.J., 2005. Modeling the impacts of anthropogenic heating on the urban climate of Philadelphia: A comparison of implementations in two PBL schemes. Atmospheric Environment 39 (1), 73–84.

Franca, G.B., Cracknell, A.P., 1994. Retrieval of land and sea surface temperature using NOAA-11 AVHRR data in north-eastern Brazil. International Journal of Remote Sensing 15 (8), 1695–1712.

Friedl, M.A., 2002. Forward and inverse modeling of land surface energy balance using surface temperature measurements. Remote Sensing of Environment 79 (2–3), 344–354.

Friedl, M.A., Davis, F.W., 1994. Sources of variation in radiometric surface temperature over a tallgrass prairie. Remote Sensing of Environment 48 (1), 1–17.

Frohn, R.C., 1998. Remote Sensing for Landscape Ecology. Lewis Publishers, Boca Raton, Florida.

Gallo, K.P., McNab, A.L., Karl, T.R., Brown, J.F., Hood, J.J., Tarpley, J.D., 1993. The use of NOAA AVHRR data for assessment of the urban heat island effect. Journal of Applied Meteorology 32 (5), 899–908.

Gallo, K.P., Owen, T.W., 1998. Assessment of urban heat island: A multi-sensor perspective for the Dallas-Ft. Worth, USA region. Geocarto International 13 (4), 35–41.

Gillespie, A.R., 1985. Lithologic mapping of silicate rocks using TIMS. In: Proceedings TIMS Data User's Workshop. Jet Propulsion Laboratory, JPL Pub. 86-38, Pasadena, California, pp. 29–44.

Gillespie, A.R., Rokugawa, S., Matsunaga, T., Cothern, J.S., Hook, S.J., Kahle, A.B., 1998. A temperature and emissivity separation algorithm for advanced spaceborne thermal emission and reflection radiometer (ASTER) images. IEEE Transactions on Geoscience and Remote Sensing 36 (4), 1113–1126.

Gillies, R.R., Carlson, T.N., 1995. Thermal remote sensing of surface soil water content with partial vegetation cover for incorporation into climate models. Journal of Applied Meteorology 34 (4), 745–756.

Gillies, R.R., Carlson, T.N., Cui, J., Kustas, W.P., Humes, K.S., 1997. A verification of the 'triangle' method for obtaining surface soil water content and energy fluxes from remote measurements of the Normalized Difference Vegetation index (NDVI) and surface radiant temperature. International Journal of Remote Sensing 18 (5), 3145–3166.

Goetz, S.J., 1997. Multisensor analysis of NDVI, surface temperature and biophysical variables at a mixed grassland site. International Journal of Remote Sensing 18 (1), 71–94.

Goward, S.N., Xue, Y., Czajkowski, K.P., 2002. Evaluating land surface moisture conditions from the remotely sensed temperature/vegetation index measurements: An exploration with the simplified biosphere model. Remote Sensing of Environment 79 (2–3), 225–242.

Grimmond, C.S.B., 2006. Progress in measuring and observing the urban atmosphere. Theoretical and Applied Climatology 84 (1–3), 3–22.

Grimmond, C.S.B., Best, M., Barlow, J., Arnfield, A.J., Baik, J.J., Baklanov, A., Belcher, S., Bruse, M., Calmet, I., Chen, F., Clark, P., Dandou, A., Erell, E., Fortuniak, K., Hamdi, R., Kanda, M., Kawai, T., Kondo, H., Krayenhoff, S., Lee, S.H., Limor, S.B., Martilli, A., Masson, V., Miao, S., Mills, G., Moriwaki, R., Oleson, K., Porson, A., Sievers, U., Tombrou, M., Voogt, J., Williamson, T., 2008. Urban surface energy balance models: Model characteristics and methodology for a comparison study. Project Report of International Urban Surface Energy Balance Model Comparison (January 2008). http://geography.kcl.ac.uk/micromet/ModelComparison/ModelComparison.pdf (Last accessed on January 22, 2009).

Grimmond, C.S.B., Oke, T.R., 1995. Comparison of heat fluxes from summertime observations in the suburbs of four North American cities. Journal of Applied Meteorology 34 (4), 873–889.

Grimmond, C.S.B., Oke, T.R., 2002. Turbulent heat fluxes in urban areas: Observations and local-scale urban meteorological parameterization scheme (LUMPS). Journal of Applied Meteorology 41 (7), 792–810.

Grimmond, C.S.B., Souch, C., 1994. Surface description for urban climate studies: A GIS based methodology. Geocarto International 9 (1), 47–59.

Hafner, J., Kidder, S.Q., 1999. Urban heat island modeling in conjunction with satellite-derived surface/soil parameters. Journal of Applied Meteorology 38 (4), 448–465.

Holt, T., Pullen, J., 2007. Urban canopy modeling of the New York city metropolitan area: A comparison and validation of single- and multilayer parameterizations. Monthly Weather Review 135 (5), 1906–1930.

Jasinski, M.F., 1990. Sensitivity of the normalized difference vegetation Index to subpixel canopy cover, soil albedo, and pixel scale. Remote Sensing of Environment 32 (2–3), 169–187.

Jiang, L., Islam, S., 2001. Estimation of surface evaporation map over southern Great Plains using remote sensing data. Water Resources Research 37 (2), 329–340.

Jiménez-Muñoz, J.C., Sobrino, J.A., 2003. A generalized single-channel method for retrieving land surface temperature from remote sensing data. Journal of Geophysical Research D: Atmospheres 108 (22), ACL 2-1- ACL 2-9.

Jiménez-Muñoz, J.C., Sobrino, J.A., 2006. Error sources on the land surface temperature retrieved from thermal infrared single channel remote sensing data. International Journal Remote Sensing 27 (5), 999–1014.

Kato, S., Yamaguchi, Y., 2005. Analysis of urban heat-island effect using ASTER and ETM+ Data: Separation of anthropogenic heat discharge and natural heat radiation from sensible heat flux. Remote Sensing of Environment 99 (1–2), 44–54.

Kealy, P.S., Gabell, A.R., 1990. Estimation of emissivity and temperature using alpha coefficients. In: Proceedings of Second TIMS Workshop. JPL Pub. 90-95, Jet Propulsion Laboratory, Pasadena, California, pp. 11–15.

Kidder, S.Q., Wu, H.T., 1987. A multispectral study of the St. Louis area under snow-covered conditions using NOAA-7 AVHRR data. Remote Sensing of Environment 22 (2), 159–172.

Kim, H.H., 1992. Urban heat island. International Journal of Remote Sensing 13 (12), 2319–2336.

Kimes, D.J., 1983. Remote sensing of row crop structure and component temperatures using directional radiometric temperatures and inversion techniques. Remote Sensing of Environment 13 (1), 33–55.

Kustas, W.P., Norman, J.M., Anderson, M.C., French, A.N., 2003. Estimating subpixel surface temperatures and energy fluxes from the vegetation index-radiometric temperature relationship. Remote sensing of Environment 85 (4), 429–440.

Lambin, F.F., Ehrlich, D., 1996. The surface temperature-vegetation index space for land use and land cover change analysis. International Journal of Remote Sensing 17 (3), 463–487.

Landsat Project Science Office,, 2002. Landsat 7 Science Data User's Handbook. Available online at: http://ltpwww.gsfc.nasa.gov/IAS/handbook/handbook_toc.html Goddard Space Flight Center, NASA, Washington, DC (last date accessed 1 February 2009).

Larson, R.C., Carnahan, W.H., 1997. The influence of surface characteristics on urban radiant temperatures. Geocarto International 12 (3), 5–16.

Liang, S., 2001. An optimization algorithm for separating land surface temperature and emissivity from multispectral thermal infrared imagery. IEEE Transactions on Geoscience and Remote Sensing 39 (2), 264–274.

Liu, H., Weng, Q., 2008. Seasonal variations in the relationship between landscape pattern and land surface temperature in Indianapolis, USA. Environmental Monitoring and Assessment 144 (1–3), 199–219.

Lo, C.P., Quattrochi, D.A., Luvall, J.C., 1997. Application of high-resolution thermal infrared remote sensing and GIS to assess the urban heat island effect. International Journal of Remote Sensing 18 (2), 287–304.

Lu, D., Weng, Q., 2006. Spectral mixture analysis of ASTER imagery for examining the relationship between thermal features and biophysical descriptors in Indianapolis, Indiana. Remote Sensing of Environment 104 (2), 157–167.

Moran, M.S., Clarke, T.R., Inoue, Y., Vidal, A., 1994. Estimating crop water deficit using the relation between surface-air temperature and spectral vegetation index. Remote Sensing of Environment 49 (3), 246–263.

Nemani, R.R., Running, S.W., 1989. Estimation of regional surface resistance to evapotranspiration from NDVI and thermal-IR AVHRR data. Journal of Applied Meteorology 28 (4), 276–284.

Nichol, J.E., 1994. A GIS-based approach to microclimate monitoring in Singapore's high-rise housing estates. Photogrammetric Engineering and Remote Sensing 60 (10), 1225–1232.

Nichol, J.E., 1996. High-resolution surface temperature patterns related to urban morphology in a tropical city: A satellite-based study. Journal of Applied Meteorology 35 (1), 135–146.

Nichol, J.E., 1998. Visualization of urban surface temperature derived from satellite images. International Journal of Remote Sensing 19 (9), 1639–1649.

Nichol, J.E., 2005. Remote sensing of urban heat islands by day and night. Photogrammetric Engineering and Remote Sensing 71 (5), 613–623.

Nishida, K., Nemani, R.R., Glassy, J.M., Running, S.W., 2003. Development of an evapotranspiration index from Aqua/MODIS for monitoring surface moisture status. IEEE Transactions on Geoscience and Remote Sensing 41 (2), 493–501.

Offerle, B., Jonsson, P., Eliasson, I., Grimmond, C.S.B., 2005. Urban modification of the surface energy balance in the west African Sahel: Ouagadougou, Burkina Faso. Journal of Climate 18 (19), 3983–3995.

Oke, T.R., 1982. The energetic basis of the urban heat island. Quarterly Journal of the Royal Meteorological Society 108 (455), 1–24.

Oke, T.R., 1988. The urban energy balance. Progress in Physical Geography 12 (4), 471–508.

Oke, T.R., Spronken-Smith, R.A., Jauregui, E., Grimmond, C.S.B., 1999. The energy balance of central Mexico City during the dry season. Atmospheric Environment 33 (24–25), 3919–3930.

Owen, T.W., Carlson, T.N., Gillies, R.R., 1998. An assessment of satellite remotely-sensed land cover parameters in quantitatively describing the climatic effect of urbanization. International Journal of Remote Sensing 19 (9), 1663–1681.

Piringer, M, Grimmond, C.S.B., Joffre, S.M., Mestayer, P., Middleton, D.R., Rotach, M.W., Baklanov, A., De Ridder, K., Ferreira, J., Guilloteau, E., Karppinen, A., Martilli, A., Masson, V., Tombrou, M., 2002. Investigating the surface energy balance in urban areas – recent advances and future needs. Water, Air and Soil Pollution: Focus 2 (5–6), 1–16.

Prata, A.J., 1993. Land surface temperatures derived from the advanced very high resolution radiometer and the along-track scanning radiometer 1: Theory. Journal of Geophysical Research 98 (D9), 16689–16702.

Prata, A.J., Caselles, V., Coll, C., Sobrino, J.A., Ottle, C., 1995. Thermal remote sensing of land surface temperature from satellites: Current status and future prospects. Remote Sensing Reviews 12 (3–4), 175–224.

Price, J.C., 1990. Using spatial context in satellite data to infer regional scale evapotranspiration. IEEE Transactions on Geoscience and Remote Sensing 28 (5), 940–948.

Qin, Z., Karnieli, A., Berliner, P., 2001. A mono-window algorithm for retrieving land surface temperature from Landsat TM data and its application to the Israel–Egypt border region. International Journal of Remote Sensing 22 (18), 3719–3746.

Quattrochi, D.A., Goel, N.S., 1995. Spatial and temporal scaling of thermal remote sensing data. Remote Sensing Review 12 (3–4), 255–286.

Quattrochi, D.A., Luvall, J.C., 1999. Thermal infrared remote sensing for analysis of landscape ecological processes: Methods and applications. Landscape Ecology 14 (6), 577–598.

Quattrochi, D.A., Ridd, M.K., 1998. Analysis of vegetation within a semi-arid urban environment using high spatial resolution airborne thermal infrared remote sensing data. Atmospheric Environment 32 (1), 19–33.

Quattrochi, D.A., Ridd, M.K., 1994. Measurement and analysis of thermal energy responses from discrete urban surface using remote sensing data. International Journal of Remote Sensing 15 (10), 1999–2022.

Rajasekar, U., Weng, Q., 2009. Urban heat island monitoring and analysis by data mining of MODIS imageries. ISPRS Journal of Photogrammetry and Remote Sensing 64 (1), 86–96.

Rao, P.K., 1972. Remote sensing of urban heat islands from an environmental satellite. Bulletin of the American Meteorological Society 53, 647–648.

Ridd, M.K., 1995. Exploring a V-I-S (Vegetation-Impervious Surface-Soil) model for urban ecosystem analysis through remote sensing: Comparative anatomy for cities. International Journal of Remote Sensing 16 (12), 2165–2185.

Roth, M., Oke, T.R., Emery, W.J., 1989. Satellite derived urban heat islands from three coastal cities and the utilisation of such data in urban climatology. International Journal of Remote Sensing 10 (11), 1699–1720.

Saitoh, T.S., Shimada, T., Hoshi, H., 1996. Modeling and simulation of the Tokyo urban heat island. Atmospheric Environment 30 (20), 3431–3442.

Sandholt, I., Rasmussen, K., Andersen, J., 2002. A simple interpretation of the surface temperature/vegetation index space for assessment of surface moisture status. Remote Sensing of Environment 79 (2–3), 213–224.

Schmid, H.P., 1988. Spatial scales of sensible heat flux variability: Representativeness of flux measurements and surface layer structure over suburban terrain. Ph.D. Thesis, The University of British Columbia, Vancouver, BC.

Schmugge, T., Hook, S.J., Coll, C., 1998. Recovering surface temperature and emissivity from thermal infrared multispectral data. Remote Sensing of Environment 65 (2), 121–131.

Small, C., 2001. Estimation of urban vegetation abundance by spectral mixture analysis. International Journal of Remote Sensing 22 (7), 1305–1334.
Smith, R.C.G., Choudhury, B.J., 1991. Analysis of normalized difference and surface temperature observations over southeastern Australia. International Journal of Remote Sensing 12 (10), 2021–2044.
Snyder, W.C., Wan, Z., Zhang, Y., Feng, Y.-Z., 1998. Classification-based emissivity for land surface temperature measurement from space. International Journal of Remote Sensing 19 (14), 2753–2774.
Sobrino, J.A., Jiménez-Muñoz, J.C., Paolini, L., 2004. Land surface temperature retrieval from LANDSAT TM 5. Remote Sensing of Environment 90 (4), 434–440.
Sobrino, J.A., Raissouni, N., 2000. Toward remote sensing methods for land cover dynamic monitoring: Application to Morocco. International Journal of Remote Sensing 21 (2), 353–366.
Steininger, M.K., 1996. Tropical secondary forest regrowth in the Amazon: Age, area and change estimation with Thematic Mapper data. International Journal of Remote Sensing 17 (1), 9–27.
Streutker, D.R., 2002. A remote sensing study of the urban heat island of Houston, Texas. International Journal of Remote Sensing 23 (13), 2595–2608.
Streutker, D.R., 2003. Satellite-measured growth of the urban heat island of Houston, Texas. Remote Sensing of Environment 85 (3), 282–289.
Tong, H., Walton, A., Sang, J., Chan, J.C.L., 2005. Numerical simulation of the urban boundary layer over the complex terrain of Hong Kong. Atmospheric Environment 39 (19), 3549–3563.
Valor, E., Cassells, V., 1996. Mapping land surface emissivity from NDVI: Application to European, African, and South American areas. Remote Sensing of Environment 57 (3), 167–184.
Voogt, J.A., Oke, T.R., 1998. Effects of urban surface geometry on remotely sensed surface temperature. International Journal of Remote Sensing 19 (5), 895–920.
Voogt, J.A., Oke, T.R., 2003. Thermal remote sensing of urban climate. Remote Sensing of Environment 86 (3), 370–384.
Watson, K., 1992. Spectral ratio method for measuring emissivity. Remote Sensing of Environment 42 (2), 113–116.
Weng, Q., 2001. A remote sensing-GIS evaluation of urban expansion and its impact on surface temperature in the Zhujiang Delta, China. International Journal of Remote Sensing 22 (10), 1999–2014.
Weng, Q., 2003. Fractal analysis of satellite-detected urban heat island effect. Photogrammetric Engineering and Remote Sensing 69 (5), 555–566.
Weng, Q., Liu, H., Lu, D., 2007. Assessing the effects of land use and land cover patterns on thermal conditions using landscape metrics in city of Indianapolis, United States. Urban Ecosystems 10 (2), 203–219.
Weng, Q., Lu, D., 2008. A sub-pixel analysis of urbanization effect on land surface temperature and its interplay with impervious surface and vegetation coverage in Indianapolis, United States. International Journal of Applied Earth Observation and Geoinformation 10 (1), 68–83.
Weng, Q., Lu, D., Liang, B., 2006. Urban surface biophysical descriptors and land surface temperature variations. Photogrammetric Engineering & Remote Sensing 72 (11), 1275–1286.
Weng, Q., Lu, D., Schubring, J., 2004. Estimation of land surface temperature-vegetation abundance relationship for urban heat island studies. Remote sensing of Environment 89 (4), 467–483.
Xian, G., Crane, M., 2006. An analysis of urban thermal characteristics and associated land cover in Tampa Bay and Las Vegas using Landsat satellite data. Remote Sensing of Environment 104 (2), 147–156.
Xiao, R., Weng, Q., Ouyang, Z., Li, W., Schienke, E.W., Zhang, W., 2008. Land surface temperature variation and major factors in Beijing, China. Photogrammetric Engineering & Remote Sensing 74 (4), 451–461.
Yang, W., Yang, L., Merchant, J.W., 1997. An analysis of AVHRR/NDVI-ecoclimatological relations in Nebraska, USA. International Journal of Remote Sensing 18 (10), 2161–2180.
Yuan, F., Bauer, M.E., 2007. Comparison of impervious surface area and normalized difference vegetation index as indicators of surface urban heat island effects in Landsat imagery. Remote Sensing of Environment 106 (3), 375–386.
Zhang, X., Aono, Y., Monji, N., 1998. Spatial variability of urban surface het fluxes estimated from Landsat TM data under summer and winter conditions. Journal of Agricultural Meteorology 54 (1), 1–11.